Mon. Not. R. Astron. Soc. **290,** 41–48 (1997)

Ultra-high-resolution observations of interstellar C_2, CH and CN towards ζ Ophiuchi and HD 169454

I. A. Crawford

Department of Physics and Astronomy, University College London, Gower Street, London WC1E 6BT

Accepted 1997 April 10. Received 1997 April 8; in original form 1997 February 12

ABSTRACT

We have used the Ultra-High-Resolution Facility (UHRF) at the Anglo-Australian Telescope (AAT), operating at a resolution of 0.33 km s^{-1} (FWHM), to observe lines arising from the five lowest rotational levels of interstellar C_2 towards ζ Ophiuchi and HD 169454. We have also obtained new observations of CH and CN towards the latter star. The very high spectral resolution has enabled us to perform a rotational excitation analysis for both of the closely spaced velocity components (separation 1.1 ± 0.1 km s^{-1}) known to be present towards ζ Oph, and, contrary to earlier results based on an analysis of only two lines, we show that these components have very similar physical conditions. In the case of HD 169454, we confirm the presence of two very closely spaced velocity components (separation 0.7 ± 0.1 km s^{-1}) in both the C_2 and the CN lines. We have determined the turbulent velocities directly from the line profiles. In all cases we find values in the range 0.23–0.45 km s^{-1}, and there is no convincing evidence for supersonic turbulence in any of the identified velocity components.

Key words: stars: individual: ζ Oph – stars: individual: HD 169454 – ISM: molecules.

1 INTRODUCTION

In an earlier paper (Crawford & Barlow 1996, hereafter Paper I) we presented ultra-high-resolution observations of the Q(2) and Q(4) lines of the (2–0) Phillips band of interstellar C_2 towards ζ Ophiuchi and HD 169454. These earlier observations enabled us to resolve the intrinsic profiles of the C_2 lines for the first time, thereby providing fairly tight constraints on the temperature and turbulence in the foreground clouds. In principle, observations of interstellar C_2 can provide additional information on the physical conditions (i.e. temperature, density and radiation field) through an analysis of the rotational excitation of the molecule (van Dishoeck & Black 1982). However, such an analysis was not possible with the earlier data, as it requires observations of the populations of a larger range of rotational levels. In order to overcome this limitation, we have now obtained additional observations, enabling us to derive the C_2 column densities for the levels $J = 0$ to 8 for both stars. These new observations have allowed us to perform an excitation analysis of the molecule, which we report in the present paper. In addition, to help further in the interpretation of the C_2 data, we have obtained new ultra-high-resolution observations of interstellar CH and CN towards HD 169454, to complement those already obtained for ζ Oph (Crawford et al. 1994).

2 OBSERVATIONS

The observations reported here were obtained with the Ultra-High-Resolution Facility (UHRF) at the Anglo-Australian Telescope in 1996 July. Observations of the R(0), Q(2), Q(4), Q(6) and Q(8) lines of the C_2 (2–0) Phillips band were obtained for ζ Oph, and the R(0), Q(6) and Q(8) lines were obtained for HD 169454 [the latter two spectral regions were found also to include the P(2) and P(4) lines]. In addition, the $R_2(1)$ (4300.313 Å) line of CH, and the R(0) and R(1) lines of the violet [$B^2\Sigma^+$–$X^2\Sigma^+$ (0–0)] band of CN near 3874 Å were observed for HD 169454. A list of the lines observed, together with the adopted rest wavelengths and oscillator strengths, is given in Table 1. A summary of the observations is given in Table 2.

The resolution, measured from the observed width of a stabilized He–Ne laser line, was 0.33 ± 0.01 km s^{-1} (FWHM), corresponding to a resolving power of $R = 910\,000$. The detector was the AAO Tektronix (1024 × 1024 24-μm pixels) CCD, and the spectrograph was operated with a confocal image slicer (Diego 1993). A post-slicer OG530 filter was used to eliminate second-order blue light from the cross-disperser. The CCD output was binned by a factor of 8 perpendicular to the dispersion direction in order to reduce the readout noise associated with extracting the broad spectrum produced by the image slicer. Other aspects of the instrument and observing procedures have been described in detail by Diego et al. (1995) and Barlow et al. (1995).

The spectra were extracted using the FIGARO data-reduction package (Shortridge 1988) at the UCL Starlink node. Scattered light was measured from the inter-order region and subtracted. Wavelength calibration was performed using a Th–Ar lamp. Once wavelength calibrated, the spectra were converted to the heliocentric velocity frame (adopting the rest wavelengths given in Table 1). Multiple exposures (Table 2) were co-added, and

Table 1. Interstellar lines observed in the present study.

Molecule	Line	λ (Å) (ref)	f (ref)
C_2	R(0)	8757.686 (1)	1.36×10^{-3} (2)
C_2	Q(2)	8761.194 (1)	6.80×10^{-4} (2)
C_2	P(2)	8766.031 (1)	1.36×10^{-4} (2)
C_2	Q(4)	8763.751 (1)	6.80×10^{-4} (2)
C_2	P(4)	8773.430 (1)	2.26×10^{-4} (2)
C_2	Q(6)	8767.759 (1)	6.80×10^{-4} (2)
C_2	Q(8)	8773.221 (1)	6.80×10^{-4} (2)
CH	$R_2(1)$*	4300.313 (3)	5.06×10^{-3} (3)
CN	R(0)†	3874.607 (3)	3.38×10^{-2} (3)
CN	R(1)‡	3873.999 (3)	2.25×10^{-2} (3)

*Split into two Λ-doublet components separated by 20.5 mÅ.
†Strictly a blend of the $R_1(0)$ and $^RQ_{21}(0)$ lines.
‡Strictly a blend of the $R_1(1)$, $R_2(1)$, and $^RQ_{21}(1)$ lines.
References: (1) van Dishoeck & de Zeeuw (1984); (2) adopting the Phillips (2–0) band oscillator strength of $f_{20} = (1.36 \pm 0.15)\times10^{-3}$ obtained by Erman & Iwamae (1995) and the Hönl–London factors tabulated by van Dishoeck & de Zeeuw (1984); (3) Black & van Dishoeck (1988).

the resulting spectra were normalized by division of low-order polynomial fits to the continua on either side of the absorption lines. The resulting spectra are shown in Figs 1 (ζ Oph), 2 and 3 (HD 169454), and we discuss each sightline separately below.

3 DISCUSSION

3.1 ζ Oph

It is now well-known that the 'main' ($-14\,\mathrm{km\,s^{-1}}$) molecular velocity component towards ζ Oph is actually a close blend of two discrete components separated by approximately $1.1\,\mathrm{km\,s^{-1}}$ (Le Bourlot, Gérin & Pérault 1989; Lambert, Sheffer & Crane 1990; Crawford et al. 1994; Barlow et al. 1995), and this structure is easily resolved in the C_2 lines presented here. Given that ζ Oph is a standard sightline for testing physical and chemical models of interstellar clouds, and that previous analyses have been based on the assumption of a single molecular cloud, it is clearly important to determine the extent to which the physical conditions in these two velocity components are different.

In order to determine the rotational excitation of each C_2 velocity component separately, least-squares Gaussian fits were performed on the observed profiles using the DIPSO spectral analysis package (Howarth, Murray & Mills 1993). Since, in reality, each of the C_2 lines from a given velocity component must have the same velocity dispersion (b-value), the number of free parameters in the fit can be reduced by forcing these to be equal. The resulting fits are shown superimposed on the observed line profiles in Fig. 1, and the corresponding line profile parameters are given in Table 3. Table 3 also gives the column densities of the $J = 0$ to 8 rotational levels, derived from the measured equivalent widths and the oscillator strengths listed in Table 1 (all of these weak lines are on the linear part of the curve of growth, despite the small b-values).

Table 2. List of observations made of interstellar lines towards ζ Oph and HD 169454. The Counts column gives the total number of continuum electrons recorded adjacent to the interstellar lines; W_λ (tot) is the total equivalent width (i.e. summed over both velocity components; 2σ errors). The 1995 observations were also reported in Paper I, but are included here for completeness.

Star	V	I	$E(B-V)$	Mol	Line	UT Date	Exposures ($n\times$s)	Counts (e^-)	W_λ (tot) (mÅ)
ζ Oph	2.6	2.5	0.33	C_2	R(0)	02-07-96 03-07-96	4×1200 2×1200	6.3×10^4	1.20 ± 0.21
					Q(2)	01-07-96 03-07-96	4×1200 3×1200	5.7×10^4	1.63 ± 0.20
					Q(4)	01-07-96	4×1200	3.2×10^4	1.41 ± 0.24
					Q(6)	02-07-96	7×1200	3.4×10^4	0.83 ± 0.22
					Q(8)	03-07-96	3×1200	3.6×10^4	0.52 ± 0.23
169454	6.6	4.8	1.14	C_2	R(0)	02-07-96	3×1200	5.2×10^3	6.23 ± 0.50
					Q(2)	20-07-95	3×1200	2.0×10^3	8.14 ± 1.18
					Q(4)	20-07-95	3×1200	2.0×10^3	3.98 ± 1.03
					Q(6); P(2)	01-07-96	6×1200	6.3×10^3	2.89 ± 0.59; 2.82 ± 0.55
					Q(8); P(4)	02-07-96	4×1200	4.1×10^3	1.28 ± 0.59; 1.68 ± 0.62
				CH	$R_2(1)$	02-07-96 03-07-96	4×1200 2×1200	1.8×10^3	25.9 ± 1.6
				CN	R(0); R(1)	03-07-96	4×1200	5.9×10^2	16.3 ± 1.6; 12.8 ± 1.5

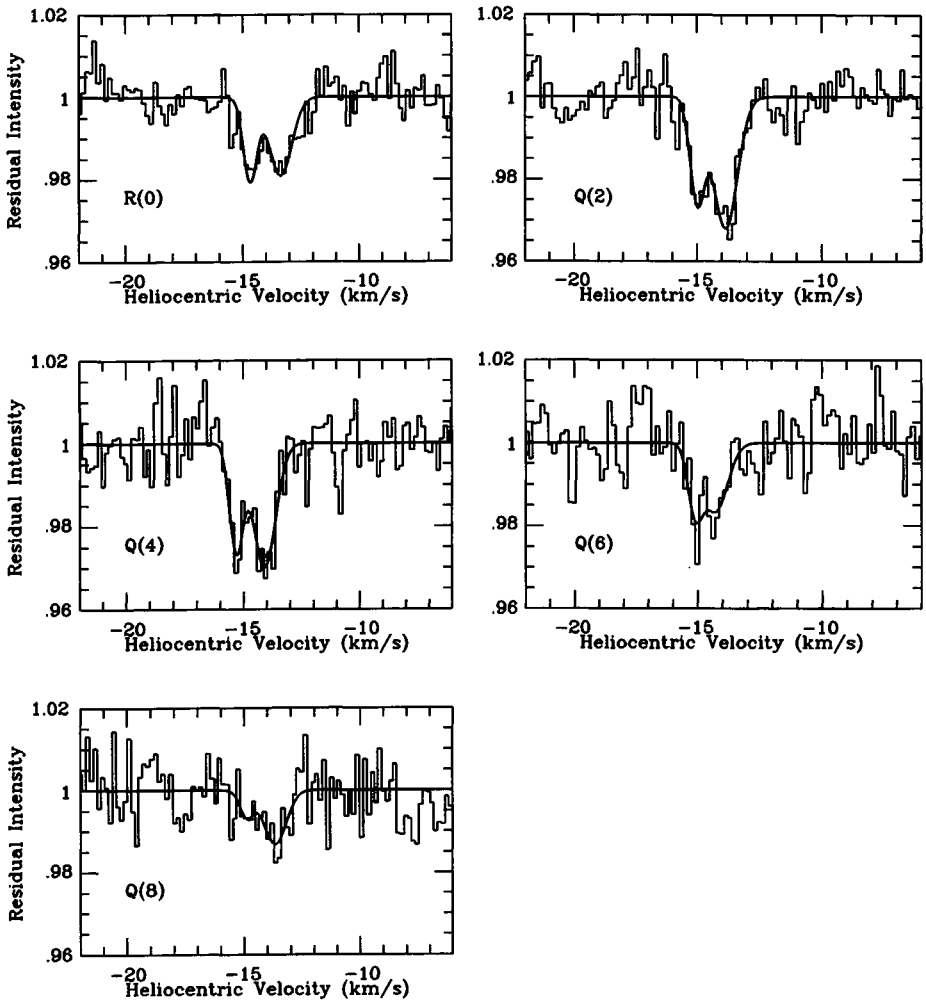

Figure 1. The interstellar C_2 lines observed towards ζ Oph. The observed data are plotted as histograms. The smooth curves are least-squares Gaussian fits with the parameters as listed in Table 3.

Table 3. Line profile parameters for the C_2 lines observed towards ζ Oph (1σ errors).

Line	$v_{\rm helio}$ (km s^{-1})	b (km s^{-1})	W_λ (mÅ)	N ($\times 10^{12}$) (cm^{-2})
R(0)	−14.7 ± 0.1	0.35 ± 0.07	0.43 ± 0.09	0.47 ± 0.10
	−13.4 ± 0.1	0.65 ± 0.08	0.68 ± 0.11	0.74 ± 0.12
Q(2)	−15.0 ± 0.1	0.35 ± 0.07	0.53 ± 0.12	1.15 ± 0.26
	−13.9 ± 0.1	0.65 ± 0.08	1.14 ± 0.13	2.47 ± 0.28
Q(4)	−15.3 ± 0.1	0.35 ± 0.07	0.54 ± 0.10	1.17 ± 0.22
	−14.1 ± 0.1	0.65 ± 0.08	1.06 ± 0.12	2.29 ± 0.26
Q(6)	−15.1 ± 0.1	0.35 ± 0.07	0.32 ± 0.10	0.69 ± 0.22
	−14.3 ± 0.1	0.65 ± 0.08	0.58 ± 0.12	1.25 ± 0.26
Q(8)	−14.9 ± 0.3	0.35 ± 0.07	0.13 ± 0.07	0.28 ± 0.15
	−13.7 ± 0.1	0.65 ± 0.08	0.47 ± 0.09	1.02 ± 0.20

Following van Dishoeck & Black (1982), we illustrate the (non-equilibrium) rotational excitation of each C_2 velocity component by plotting the quantity $-\log_e[5N_J/(2J+1)N_2]$ against $\Delta E/k$. Here, N_J is the column density of level J and N_2 the column density of $J=2$, ΔE is the energy difference between level J and $J=2$, and k is Boltzmann's constant. In these plots, a Boltzmann distribution at temperature T is represented by a straight line with gradient $1/T$, and non-equilibrium excitation is revealed by departure from this line. These diagrams for the two velocity components towards ζ Oph are shown in Fig. 4.

Detailed non-equilibrium calculations of the excitation of interstellar C_2, allowing for radiative and collisional excitation/de-excitation, and fluorescence in the interstellar radiation field, have been computed by van Dishoeck & Black (1982) and van Dishoeck (1984). The populations are governed by three parameters, the kinetic temperature, T_k, the space density of collision partners, n_c [$\equiv n(H) + n(H_2)$], and a scaling factor for the interstellar radiation field, I, near a wavelength of 1 μm (where C_2 is most sensitive to radiative excitation). In addition, the excitation depends on the cross-section for collisional de-excitation, σ_0, which is currently uncertain by a factor of about 2. Tables giving the column density ratios N_J/N_2 as a function of both T_k and the

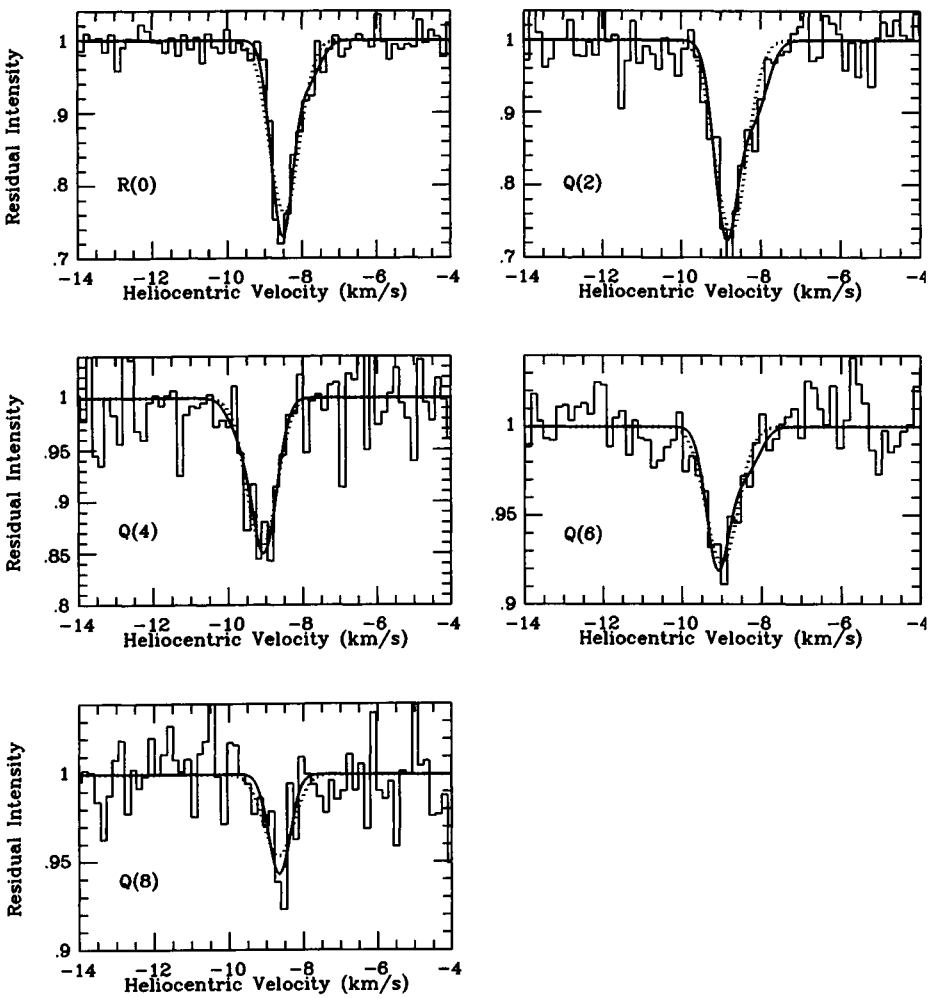

Figure 2. The interstellar C_2 lines observed towards HD 169454. The observed data are plotted as histograms. The smooth curves are least-squares Gaussian fits with the parameters listed in Table 5. The dotted curves are single-component fits, while the solid curves are the preferred two-component fits (see text).

combined parameter $n_c\sigma_0/I$ have been compiled by van Dishoeck (1984, pp. 258–259). We note that although the (2–0) band oscillator strength adopted here ($1.36 \pm 0.15 \times 10^{-3}$) is 20 per cent smaller than the value (1.67×10^{-3}) used by van Dishoeck (1984) this difference, which is in any case small compared with the other uncertainties, is offset by the fact that the local interstellar radiation field at 1 μm (6×10^5 photon s^{-1} cm^{-2} $Å^{-1}$: Mathis, Mezger & Panagia 1983) is larger than the value adopted by van Dishoeck (1984) by a similar factor [cf. section II(e) of van Dishoeck & Black 1989]. We have therefore adopted the models of van Dishoeck (1984) for the interpretation of the C_2 data presented here, with the understanding that the scaling factor for the interstellar radiation field, I, is with respect to the solar neighbourhood value of 6×10^5 near-IR photon s^{-1} cm^{-2} $Å^{-1}$ obtained by Mathis et al. (1983).

Fig. 4 shows the results of this analysis for the two C_2 velocity components towards ζ Oph, and the corresponding values of T and $n_c\sigma_0/I$ are summarized in Table 4. We obtain best-fitting temperatures of 20 and 30 K for the −15.0 and −13.9 km s^{-1} components respectively, with $n_c\sigma_0/I = 5 \times 10^{-14}$ cm^{-1} in each case. Adopting $\sigma_0 = 2 \times 10^{-16}$ cm^2 (van Dishoeck & Black 1989), and $I = 1$, this yields a density of $n_c = 250$ cm^{-3} for both velocity components. Allowing for the uncertainties in these quantities, we see that, contrary to the tentative conclusions of Paper I, there is no evidence that the two velocity components have significantly different temperatures or densities. Indeed, the temperatures obtained for both components individually are essentially identical to the value ($T_k = 30 \pm 10$ K) obtained from an analysis of the (3–0) band by van Dishoeck & Black (1986), and *Hubble Space Telescope* observations of the Mulliken (0–0) band at 2313 Å by Lambert, Sheffer & Federman (1995), where the velocity sub-structure was not resolved.

Measurement of the intrinsic velocity dispersions (b-values) of interstellar lines provides additional information on the temperature and turbulence within the absorbing clouds, and this is also summarized in Table 4. We stress that, as the UHRF has fully resolved these line profiles, the tabulated b-values are well-determined, in spite of their low values. We also note that the low velocity dispersions obtained here for the C_2 lines are similar to those found for the CN components (Lambert et al. 1990; Crawford et al. 1994) and for the CO emission lines (Le Bourlot et al. 1989), towards this star.

The velocity dispersion parameter, b, is related to the kinetic temperature of the gas, T_k, and the rms turbulent velocity along the line of sight, v_t, through the expression

$$b = \left(\frac{2kT_k}{m} + 2v_t^2\right)^{1/2}, \quad (1)$$

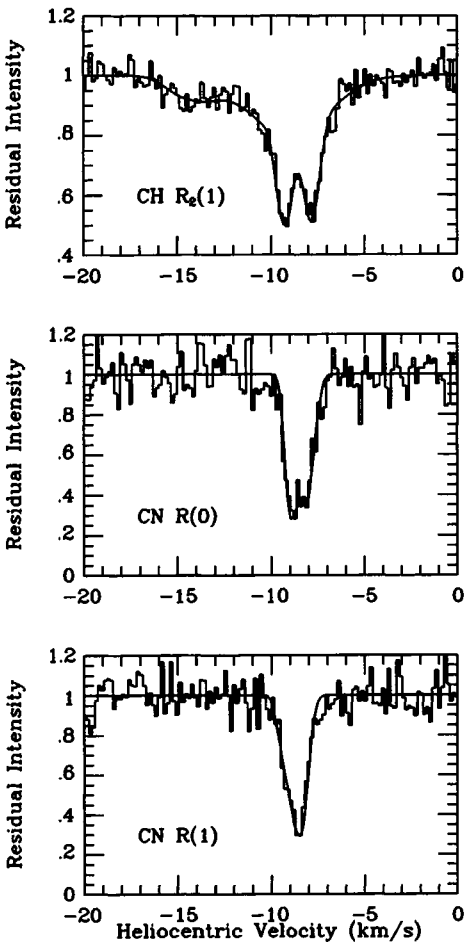

Figure 3. The interstellar CH and CN lines observed towards HD 169454. The observed data are plotted as histograms. The smooth curves are theoretical line profiles with the parameters given in Table 6.

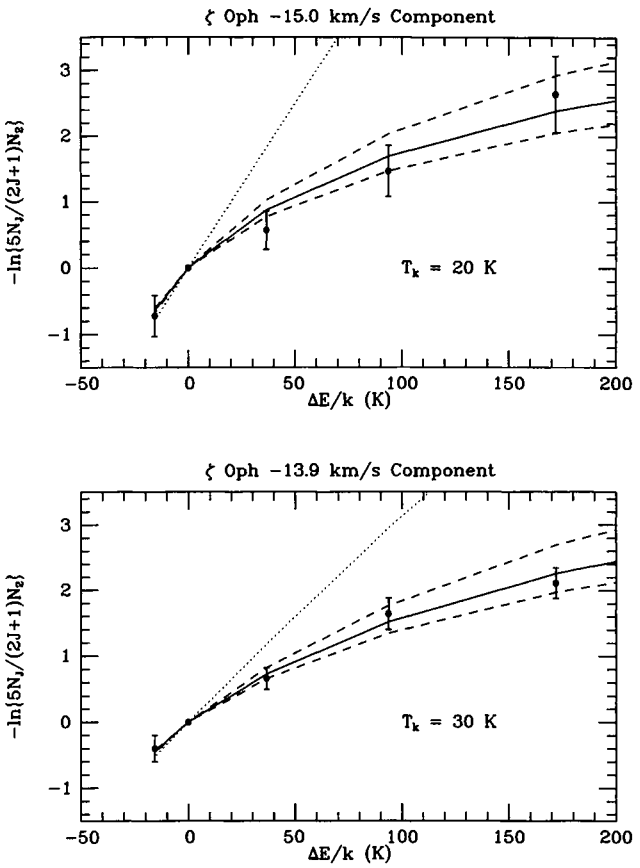

Figure 4. Relative rotational-level populations of C_2 with respect to $J = 2$, as a function of excitation potential, for the two velocity components observed towards ζ Oph. The solid curves give the theoretical populations at the indicated temperatures for $n_c\sigma_0/I = 5\times10^{-14}$ cm^{-1} (van Dishoeck 1984). In both cases the dashed curves give the theoretical populations obtained with $n_c\sigma_0/I = 4\times10^{-14}$ cm^{-1} (lower curve) and 7×10^{-14} cm^{-1} (upper curve). The dotted lines give the thermal populations at these temperatures.

Table 4. Summary of results obtained from the C_2 lines. b is the velocity dispersion of each identified velocity component; T_k^{ul} is the corresponding upper limit to the kinetic temperature (based on the assumption that turbulence does not contribute to the observed linewidths); T_k and n_c are the kinetic temperatures and densities of collision partners based on the rotational level populations; v_t is the the rms turbulent velocity, and C_s is the sound speed, corresponding to this kinetic temperature.

Star	v_{helio} (km s^{-1})	b (km s^{-1})	T_k^{ul} (K)	T_k (K)	$n_c\sigma_0/I$ (cm^{-1})	n_c (cm^{-3})	v_t (km s^{-1})	C_s (km s^{-1})
ζ Oph	−15.0	0.35 ± 0.07	180 ± 70	20^{+20}_{-10}	$5^{+15}_{-1}\times10^{-14}$	250^{+750}_{-50}	0.23 ± 0.05	$0.27^{+0.11}_{-0.08}$
	−13.9	0.65 ± 0.08	610 ± 150	30^{+20}_{-10}	$5^{+5}_{-1.5}\times10^{-14}$	250^{+250}_{-75}	0.45 ± 0.06	$0.33^{+0.09}_{-0.06}$
HD 169454	−8.7	0.54 ± 0.03	420 ± 50	15^{+5}_{-5}	$8^{+2}_{-2}\times10^{-14}$	400^{+100}_{-100}	0.38 ± 0.02	$0.23^{+0.04}_{-0.04}$
HD 169454*	−8.8	0.36 ± 0.03	190 ± 20	15^{+5}_{-5}	$7^{+1}_{-2}\times10^{-14}$	350^{+50}_{-100}	0.24 ± 0.02	$0.23^{+0.04}_{-0.04}$
	−8.1	0.44 ± 0.07	280 ± 60	30^{+30}_{-10}	$10^{+\infty}_{-3}\times10^{-14}$	$500^{+\infty}_{-150}$	0.29 ± 0.06	$0.33^{+0.13}_{-0.06}$

*Assuming two velocity components separated by 0.7 km s^{-1} (see text).

Table 5. Line profile parameters for the C_2 lines observed towards HD 169454 (1σ errors). For each line, the first (underlined) entry is based on the assumption of a single velocity component (dotted curves in Fig. 2), and the next two entries give the values obtained by fitting two components, separated by 0.7 km s^{-1}, to the observed profiles (solid curves in Fig. 2).

Line	$v_{\rm helio}$ (km s^{-1})	b (km s^{-1})	W_λ (mÅ)	N ($\times 10^{12}$) (cm^{-2})
R(0)	−8.5 ± 0.1	0.54 ± 0.03	7.03 ± 0.41	7.62 ± 0.44
	−8.5 ± 0.1	0.36 ± 0.03	5.61 ± 0.43	7.01 ± 0.56
	−7.8 ± 0.1	0.44 ± 0.07	1.34 ± 0.46	1.45 ± 0.50
Q(2)	−8.7 ± 0.1	0.54 ± 0.03	7.83 ± 0.44	18.83 ± 1.35
	−8.9 ± 0.1	0.36 ± 0.03	5.60 ± 0.47	13.90 ± 1.23
	−8.2 ± 0.1	0.44 ± 0.07	2.57 ± 0.54	5.85 ± 1.24
Q(4)	−9.1 ± 0.1*	0.54 ± 0.03	4.27 ± 0.39	9.88 ± 0.90
	−9.7 ± 0.1	0.36 ± 0.03	0.53 ± 0.45	1.14 ± 0.97
	−9.0 ± 0.1	0.44 ± 0.07	3.70 ± 0.51	8.55 ± 1.20
Q(6)	−9.0 ± 0.1	0.54 ± 0.03	2.26 ± 0.38	5.10 ± 0.84
	−9.1 ± 0.1	0.36 ± 0.03	1.65 ± 0.39	3.56 ± 0.84
	−8.4 ± 0.1	0.44 ± 0.07	0.63 ± 0.46	1.36 ± 1.00
Q(8)	−8.7 ± 0.1	0.54 ± 0.03	1.38 ± 0.37	2.98 ± 0.80
	−8.6 ± 0.1	0.36 ± 0.03	1.21 ± 0.31	2.52 ± 0.67
	....	....	≤0.80	≤1.73

*Velocity uncertain due to the detection of only one comparison line in the Th–Ar comparison lamp spectrum.

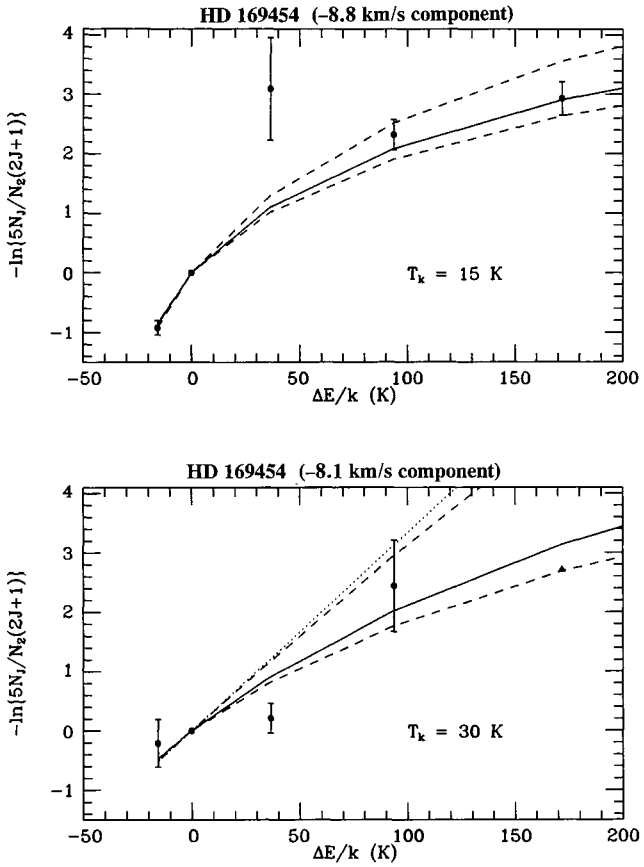

Figure 5. Relative rotational-level populations of C_2 for the cloud towards HD 169454, assuming two velocity components (solid curves in Fig. 2). For the −9.0 km s^{-1} component, the solid curve gives the theoretical populations at $T_{\rm k} = 15$ K and $n_{\rm c}\sigma_0/I = 7\times10^{-14}$ cm^{-1}; the lower and upper dashed curves correspond to $n_{\rm c}\sigma_0/I = 6\times10^{-14}$ and 10×10^{-14} cm^{-1}, respectively. For the −8.4 km s^{-1} component, the solid curve gives the theoretical populations at $T_{\rm k} = 30$ K and $n_{\rm c}\sigma_0/I = 10\times10^{-14}$ cm^{-1}; the lower and upper dashed curves correspond to $n_{\rm c}\sigma_0/I = 7\times10^{-14}$ cm^{-1} and 10^{-12} cm^{-1}, respectively. The dotted lines give the thermal populations at the indicated temperatures.

where k is Boltzmann's constant and m is the mass of the atom or ion observed. Equation (1) may be used to derive a rigorous upper limit to the kinetic temperature, $T_{\rm k}^{\rm ul}$, by assuming $v_{\rm t} = 0$, and these values are listed in Table 4. Now that we have derived values for $T_{\rm k}$ from the excitation analysis, it is possible to insert these into equation (1) and derive $v_{\rm t}$ directly, and these values are also given in the table.

As discussed in Paper I, it is of particular interest to determine whether or not these turbulent velocities are supersonic. The last column of Table 4 gives the speed of sound for the temperatures obtained from the C_2 excitation analysis, on the assumption of a molecular hyrdogen gas containing 10 per cent helium by number (note that if half the hydrogen nuclei were actually in atomic form, the sound speeds would be roughly 18 per cent higher). We see that for both components the turbulent velocities are comparable to the sound speeds, and, in the case of the −13.9 km s^{-1} component, apparently somewhat higher. Nevertheless, given the quoted errors, and recognizing that the presence of non-molecular hydrogen will raise the sound speed above the tabulated values, it seems clear that there is no compelling case for supersonic turbulence in either of the C_2 velocity components towards ζ Oph. We should perhaps note that the referee has suggested that the two velocity components might themselves be due to coherent motions arising from the long-wavelength tail of a Kolmogorov-type turbulent velocity distribution within a single cloud. However, this possibility appears to be ruled out by the CO map reported by Barrett, Soloman & Mooney (1989), which strongly favours the interpretation that these components arise in two discrete foreground clouds.

3.2 HD 169454

The diffuse molecular cloud towards HD 169454 has been studied in detail by Jannuzi et al. (1988). It has a diameter of 20 arcmin (corresponding to 0.7 pc at an estimated distance of 125 pc), and the CO maps reveal the presence of three relatively dense clumps, each approximately 0.15 pc across, connected by lower intensity emission. The line of sight to HD 169454 passes approximately 5.7 arcmin (0.21 pc) south-south-west of the centre of one of these clumps (clump B in fig. 1 of Jannuzi et al. 1988).

Fig. 2 shows the C_2 lines observed towards HD 169454 [where the Q(2) and Q(4) lines reported previously in Paper I have been included for completeness]. The dotted and solid curves in Fig. 2 show least-squares Gaussian fits to the observed profiles under the assumption of one and two velocity components, respectively (see below).

A C_2 rotational analysis of this line of sight was carried out by van Dishoeck & Black (1989), on the basis of which which they

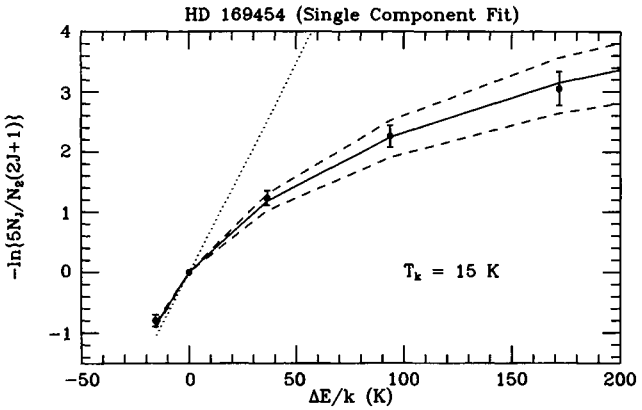

Figure 6. Relative rotational-level populations of C_2 with respect to $J = 2$ for the cloud towards HD 169454, under the assumption of a single velocity component (dotted curves in Fig. 2). The solid curve give the theoretical populations for a temperature of 15 K and $n_c\sigma_0/I = 8 \times 10^{-14}$ cm^{-1} (van Dishoeck 1984). The dashed curves give the populations obtained with $n_c\sigma_0/I = 6 \times 10^{-14}$ cm^{-1} (lower curve) and 10×10^{-14} cm^{-1} (upper curve). The dotted line gives the thermal population at 15 K.

Table 6. Line profile parameters for the CH and CN lines observed towards HD 169454.

Line	$v_{\rm helio}$ (km s^{-1})	b (km s^{-1})	log N (cm^{-2})
CH $R_2(1)$	-14.2 ± 0.2	$1.20^{+0.30}_{-0.40}$	$12.60^{+0.10}_{-0.20}$
	-9.1 ± 0.2	$2.80^{+1.20}_{-0.80}$	$13.30^{+0.20}_{-0.20}$
	-8.6 ± 0.1	$0.55^{+0.05}_{-0.05}$	$13.22^{+0.13}_{-0.07}$
CN R(0)	-9.0 ± 0.1	$0.30^{+0.15}_{-0.10}$	$12.40^{+0.10}_{-0.15}$
	-8.2 ± 0.1	$0.45^{+0.20}_{-0.15}$	$12.43^{+0.12}_{-0.13}$
CN R(1)	-9.4 ± 0.1	$0.30^{+0.10}_{-0.10}$	$12.05^{+0.25}_{-0.35}$
	-8.6 ± 0.1	$0.45^{+0.20}_{-0.20}$	$12.70^{+0.10}_{-0.10}$

deduced a very low kinetic temperature of 15^{+10}_{-5} K. This temperature was derived under the assumption of a single velocity component and, as for the ζ Oph sightline, it is of interest to see how this conclusion is affected by the presence of multiple velocity structure. In order to check our results against those of van Dishoeck & Black, we first fitted a single Gaussian velocity component to the observed C_2 line profiles (dotted curves in Fig. 2), and used the equivalent widths obtained from these single-component fits to derive the column densities listed in Table 5 (underlined entries). In these fits, the b-values were constrained to be equal, as they must be in practice, and this is the reason why the equivalent widths of the resulting Gaussians differ somewhat from the 'raw' equivalent widths listed in Table 1. For these relatively strong, and very narrow, lines, there is a significant degree of saturation, and the column densities were obtained from a curve of growth appropriate for the measured b-value (0.54 ± 0.03 km s^{-1}), which increases the column densities derived from the strongest lines by about 10 per cent.

Fig. 6 shows the results of the rotational excitation analysis under the assumption of a single velocity component, and the derived temperature and density are given in Table 4. It will be seen that this analysis yields exactly the same kinetic temperature, 15 ± 5 K, obtained by van Dishoeck & Black (1989) from their completely independent set of observations. As noted in Paper I, this low temperature, combined with the measured linewidths, implies a mildly supersonic value of v_t (cf. Table 4).

In Paper I we drew attention to evidence that the Q(2) line towards HD 169454 may be composed of two discrete velocity components, separated by 0.7 ± 0.1 km s^{-1}. This structure is also found here in the R(0) and Q(6) lines (Fig. 2, Table 5), and in the CN lines with an essentially identical velocity separation (see below). Thus there seems to be no doubt that the part of the cloud sampled by the line of sight to HD 169454 cloud contains two discrete molecular condensations ('clumps') with radial velocities differing by $\approx$0.7 km s^{-1}. This is consistent with the complicated internal structure mapped in CO by Jannuzi et al. (1988).

Given this evidence for multiple velocity structure, we have fitted the observed line profiles with two velocity components separated by 0.7 km s^{-1} (solid curves in Fig. 2). As before, we constrained the b-values of each velocity component to be equal. The resulting line-profile parameters are given in Table 5 (non-underlined entries). Fig. 5 shows the results of performing a rotational analysis for each of the two velocity components separately, and the results are summarized in Table 4. It will be seen that there is marginal evidence for the weaker ('-8.1 km s^{-1}') component having a slightly higher kinetic temperature, and a higher density, than the stronger ('-8.8 km s^{-1}') component. In any case, it is clear that the presence of two velocity components removes the need to postulate supersonic turbulence in this cloud.

Fig. 3 shows the CH and CN line profiles towards HD 169454. For these quite strongly saturated lines, the line profile parameters were obtained by means of the interstellar line-profile modelling routines in the DIPSO spectral analysis package (Howarth et al. 1993). The resulting fits are indicated by solid curves in Fig. 3, and the parameters (heliocentric velocities, b-values, and column densities) deduced from them are listed in Table 6. In fitting these profiles, the Λ-doublet structure in CH, and the fine rotational splitting in CN, has been included (cf. footnote to Table 1).

Both CN lines are well fitted with two very narrow velocity components, separated by 0.8 ± 0.1 km s^{-1}, which is fully consistent with the asymmetries observed in the C_2 lines. In the case of CH, although a total of three velocity components were identified (Table 6), only one of these ($v_{\rm helio} = -8.6$ km s^{-1}) is as comparably narrow as the CN and C_2 lines (the obvious double structure present in CH, with a velocity separation of 1.4 km s^{-1}, is due to the Λ-doubling in this one narrow component and not to additional velocity structure). The b-value obtained for this narrow CH component (0.55 ± 0.05 km s^{-1}) is consistent with it having formed in the same internal clump as one or other of the C_2 and CN components ($T_k \approx 20$ K, $v_t \approx 0.3$ km s^{-1}).

The other two CH components are much broader (Table 6). In particular, in order to fit the wings of the narrow CH component, a broad ($b = 2.8^{+1.2}_{-0.8}$ km s^{-1}) component, with a central velocity very similar to that of the narrow component, is found to be necessary. A similar broad CH component was found in the case of ζ Oph (Lambert et al. 1990; Crawford et al. 1994), which is interpreted as arising in a warm and/or turbulent envelope surrounding the cool cores that give rise to the narrow lines. In the case of HD 169454, a common molecular envelope that surrounds denser internal condensations is strongly suggested by the CO maps of Jannuzi et al. (1988). It is not clear how to incorporate the third (-14.2 km s^{-1}) CH component into a consistent model of the HD 169454 cloud,

and it seems likely that this arises in a separate diffuse molecular cloud somewhere along the 1700-pc line of sight to the star (Humphreys 1978).

4 CONCLUSIONS

We have observed the R(0), Q(2), Q(4), Q(6) and Q(8) lines of the (2–0) Phillips band of interstellar C_2 towards ζ Oph and HD 169454 using the UHRF at the AAT. In addition, we have observed the CH $R_2(1)$ and CN R(0) and R(1) lines towards HD 169454, to complement previously published UHRF observations of these lines towards ζ Oph. The spectral resolution (0.33 km s^{-1} FWHM) enabled us to resolve fully the intrinsic line profiles, and thereby obtain accurate values for the intrinsic velocity dispersions (b-values). In all cases, the C_2 and CN lines were found to be extremely narrow, with b-values in the range 0.35 to 0.65 km s^{-1}.

In the case of ζ Oph, both of the previously known velocity components (separation 1.1 ± 0.1 km s^{-1}) were resolved in all the C_2 lines, and this enabled us to perform a rotational excitation analysis for each component separately. Contrary to the tentative results reported in Paper I, which were based on an analysis of only two lines, we find that both of these components are described by similar physical conditions ($T_k \approx 30$ K; $n_c \approx 250$ cm^{-3}; $v_t \approx 0.2$–0.4 km s^{-1}; Table 4). Although one of these components appears to have a turbulent velocity marginally in excess of the sound speed for pure molecular hydrogen gas (Table 4), allowance for the quoted 1σ errors, and the fact that an admixture of atomic hydrogen would increase the sound speed, leads us to conclude that there is no evidence for supersonic turbulence in either of these velocity components.

In the case of HD 169454, we confirm the very low temperature ($T_k = 15$ K) obtained by van Dishoeck & Black (1989) on the basis of a single velocity component (Table 4). However, we note that the asymmetries present in the R(0), Q(2) and Q(6) C_2 line profiles, and the clearly double structure of the CN lines, strongly suggests that the line of sight has intercepted two clumps of dense molecular gas within the cloud, separated by 0.7 ± 0.1 km s^{-1}. This is consistent with the cloud structure determined from CO observations by Jannuzi et al. (1988). By fitting the C_2 lines with two velocity components separated by 0.7 km s^{-1}, we find that both clumps are described by similar physical conditions, although there is marginal evidence that the weaker component is somewhat hotter and denser than the stronger component (Table 4).

Finally, we note that these results strictly apply only to those regions of the clouds where the C_2 molecule occurs. There is considerable theoretical and observational evidence (discussed by Crawford 1995, and references therein) that diffuse molecular clouds have a stratified structure, with different molecules tracing different regions. In particular, the observation that turbulence is subsonic in the denser regions, where C_2 is thought to form, does not necessarily imply that this is true in the outer regions bordering the intercloud medium.

ACKNOWLEDGMENTS

I thank PATT for the award of telescope time, and PPARC for financial support. I am grateful to M. J. Barlow for advice and encouragement, and to the referee for helpful comments on the original manuscript.

REFERENCES

Barlow M. J., Crawford I. A., Diego F., Dryburgh M., Fish A. C., Howarth I. D., Spyromilio J., Walker D. D., 1995, MNRAS, 272, 333
Barrett J. W., Solomon P. M., Mooney T. J., 1989, BAAS, 21, 761
Black J. H., van Dishoeck E. F., 1988, ApJ, 331, 986
Crawford I. A., 1995, MNRAS, 277, 458
Crawford I. A., Barlow M. J., 1996, MNRAS, 280, 863 (Paper I)
Crawford I. A., Barlow M. J., Diego F., Spyromilio J., 1994, MNRAS, 266, 903
Diego F., 1993, Appl. Opt., 32, 6284
Diego F. et al., 1995, MNRAS, 272, 323
Erman P., Iwamae A., 1995, ApJ, 450, L31
Howarth I. D., Murray J., Mills D., 1993, Starlink User Note, No. 50
Humphreys R. M., 1978, ApJS, 38, 309
Jannuzi B. T., Black J. H., Lada C. J., van Dishoeck E. F., 1988, ApJ, 332, 995
Lambert D. L., Sheffer Y., Crane P., 1990, ApJ, 359, L19
Lambert D. L., Sheffer Y., Federman S. R., 1995, ApJ, 438, 740
Le Bourlot J., Gérin M., Pérault M., 1989, A&A, 219, 279
Mathis J. S., Mezger P. G., Panagia N., 1983, A&A, 128, 212
Shortridge K., 1988, Starlink User Note, No. 86
van Dishoeck E. F., 1984, PhD Thesis, Univ. of Leiden
van Dishoeck E. F., Black J. H., 1982, ApJ, 258, 533
van Dishoeck E. F., Black J. H., 1986, ApJ, 307, 332
van Dishoeck E. F., Black J. H., 1989, ApJ, 340, 273
van Dishoeck E. F., de Zeeuw T., 1984, MNRAS, 206, 383

This paper has been typeset from a TEX/LATEX file prepared by the author.